LA-UR-74-629

LA-UR-74-629

96,531

TITLE: A COMPARATIVE ANALYSIS OF D-T FUSION REACTOR RADIOACTIVITY AND AFTERHEAT

Conf-740402--18

AUTHOR(S): Donald J. Dudziak
R. A. Krakowski

SUBMITTED TO: "First Topical Meeting on the Technology of Controlled Nuclear Fusion" to be held in San Diego April 16-18, 1974. To be published in Proceedings of meeting.

los alamos
scientific laboratory
of the University of California
LOS ALAMOS, NEW MEXICO 87544

m No. 836
No. 2629

UNITED STATES
ATOMIC ENERGY COMMISSION
CONTRACT W-7405-ENG. 36

A COMPARATIVE ANALYSIS OF D-T FUSION REACTOR RADIOACTIVITY AND AFTERHEAT

Donald J. Dudziak and R. A. Krakowski
University of California, Los Alamos Scientific Laboratory
Los Alamos, New Mexico 87544

ABSTRACT

Induced radioactivity and afterheat in fusion reactor blanket structures and magnetic coils are essential inputs for environmental impact studies. These quantities have been calculated for a Reference Theta-Pinch Reactor (RTPR) and compared with reported results for other fusion reactors and typical fast fission reactors. Major independent variables considered in the RTPR analysis were structural material (Nb-1%Zr,V-20%Ti), neutron wall loading (0.2 to 6.7 MW/m^2), operating time (1 to 20 y) and time after shutdown (0 to 30 000 y). For a given operating time, large radioactivity contributions from ^{95}Nb render higher Ci/Wt and Ci/Wt y values at higher wall loadings and < 1 y after shutdown. At long times after shutdown this dependence is reversed and represents an advantage relative to long-term radwaste storage. Activity from V-20%Ti is very insensitive to wall loading or operating time. For either material, afterheat power densities are about two orders-of-magnitude lower than for fission reactors.

1. Introduction

The major short and long-term radiological impact of fusion power reactors as envisioned today is associated with the large inventories of tritium and the neutron activation of structural components of the blanket. The mechanisms and radiological implications of tritium release to the environment have been treated in detail for the Reference Theta-Pinch Reactor (RTPR) design[1] and are not considered here. The impact of structural activation is made on both short-term (accidents, maintenance) and long-term (radstorage, blanket processing) radioactivity as well as nuclear afterheat (loss-of-cooling). The major independent variables considered by this study are structural material (Nb-1%Zr, V-20%Ti), 14.1-MeV neutron wall loading (I_w = 0.2 to 6.7 MW/m^2), operating time (T = 1 to 20 y), and the time after shutdown (t_s = 0 to 30 000 y). Although the calculational results presented herein are based on the RTPR design,[2] comparisons are made with fission reactors and other fusion reactor designs. Calculational results are analyzed in terms of activation per unit energy generated, Q(Ci/Wt y);* activation per unit power, A(Ci/Wt); biological hazard potential, BHP(km^3/Wt); and fraction of operating power represented by nuclear afterheat, P/P_o. This study emphasized Nb-1%Zr structural alloy, although V-20%Ti is also considered.** Activation of the copper magnet coils used in the RTPR design is also included for the Nb-1%Zr case, and should differ little for V-20%Ti.

Afterheat and radioactivity calculations for several D-T fusion reactor designs have been published.[3-10] Differences observed among afterheat and radioactivity calculations result largely from design differences, since fusion reactor afterheat and radioactivity are intrinsically dependent upon the blanket design and operating conditions. Typical blanket parameters which strongly influence induced activity levels calculated by various design groups are (i) first-wall neutron loading (~ 0.1 to 10 MW/m^2); (ii) volume percent of structural material in the blanket (1 to 6 v/o); (iii) neutron moderating material (graphite or stainless steel) and its location relative to high flux regions; and (iv) projected useful lifetime of the structure (5-20 y). These parameters determine the relative amounts of specific radioisotopes generated and their time-dependent decay. In contrast, afterheat for fission reactors is weakly design dependent.

The neutron activation of structural material in any D-T fusion reactor power plant presents a three-fold problem:

i) in event of a loss-of-coolant accident the nuclear decay heat will result in an increased blanket temperature, leading perhaps to melting of a portion of the structural metal.

ii) radioactive structural material conceivably may be released in the form of flocculent oxides, along with activated coolant, during the course of a severe liquid-metal fire.

iii) the necessity to periodically replace and perhaps recycle reactor structural material creates a significant radwaste disposal/storage/handling problem.

---

*Thermal power output in watts is abbreviated as Wt.

**While advantageous from the viewpoint of long-term radioactivity and afterheat, V-20%Ti has strength and corrosion (oxygen) limitations when used as a high-temperature (> 900 K) structural material.

Fission reactor power plants share similar problems, except that the demands imposed by nuclear afterheat, the potential for accidental radioactivity releases, and radwaste management are almost entirely associated with fission products and transuranium elements.

2. Calculational Models

The evolution of a conceptual theta-pinch reactor design[11,12,13,2] has included successive neutronic analyses.[14,15] The toroidal reactor power plant has an aspect ratio of 1|2 and is composed of 2-metre long modules with 100 radial segments per module.[2] Except for the radial walls (1 mm Nb and 0.3 mm Al_2O_3) which separate the 100 segments around the minor circumference, the blanket can be represented by a series of concentric cylinders. Blanket schematic drawings and neutronic models can be found in Refs. 2, 15 and 16. Niobium/alumina walls were all taken into account either explicitly or by homogenization in the neutronic model, and the total blanket inventory of niobium structure, therefore, is realistically represented. Accounting for metal structure within regions such as the graphite moderator is especially important because a large proportion of thermal captures occur in moderating regions. No attempt was made to alter the structural design for V-20%Ti; rather, the alloy was simply substituted for niobium in activation calculations.

All transport calculations were performed with the DTF-IV discrete ordinates code,[17] using cross sections from the standard LASL/CTR 100-group library.[18] Activation cross sections were obtained from various sources, including ENDF, the "barn book",[19] and nuclear model calculations.[18] In particular, multigroup cross sections for excitation of ^{93m}Nb, the 12-year metastable state of ^{93}Nb, were derived from the work of Hegedus.[20] Because of its dominant contribution, production of ^{95}Nb via the $^{94}Nb(n,\gamma)\ ^{95}Nb$ reaction introduces the greatest uncertainty in calculations of both radioactivity and afterheat from niobium. The cross section for this reaction has not been thoroughly measured; both the thermal cross section and the resonance integral have been found to be approximately 15 times the respective values for the $^{93}Nb(n,\gamma)\ ^{94}Nb$ reaction.[21] Therefore, the assumption was made[18] that the $^{94}Nb(n,\gamma)\ ^{95}Nb$ cross section is everywhere 15 times that for $^{93}Nb(n,\gamma)\ ^{94}Nb$. This assumption should be conservative (i.e., overpredict ^{95}Nb and ^{95m}Nb activity in most cases) unless the ^{94}Nb resonances are predominantly at higher energies* than those in ^{93}Nb. Another effect tending to make the $^{95,95m}Nb$ production calculations conservative is resonance self-shielding. Accounting for resonance self-shielding in ^{93}Nb has been estimated[15] to reduce the ^{94}Nb production by ~ 20%, while this effect in ^{94}Nb resonance capture is fluence-dependent and indeterminate. Resonance self-shielding was ignored with the intention of providing conservative results for $^{95,95m}Nb$. However, long-term ^{94}Nb activity may still be underpredicted because of overestimating burnout.

The branching ratio to ^{95m}Nb in the $^{94}Nb(n,\gamma)$ reaction was assumed[18] to be 0.2, and 0.5 was assumed[18] for the $^{93}Nb(n,\gamma)$ reaction to ^{94m}Nb and ^{94}Nb. As a conservative assumption all $^{93}Nb(n,\alpha)$ reactions were assumed to branch to ^{90m}Y. Activation of the metastable state of ^{92}Nb has the cross section originally given (erroneously) in the ENDF-II data file for the $^{93}Nb(n,2n)$ reaction. For $I_w = 2.0$ and 6.7 MW/m^2 the production of ^{92}Zr by ^{92m}Nb decay exceeded the naturally occurring ^{92}Zr in Nb-1%Zr by factors of 8 and 26 at T = 5 y, indicating that the ^{89}Sr activity per unit operating power will be a strong function of both wall loading and operating time, which is similar to $^{95,95m}Nb$ behavior. Likewise, ^{90}Sr, which results mostly from successive reactions via ^{93}Zr, has the same strong dependence. The contribution from $^{94}Zr(n,n'\alpha)$ reactions is

*Fragmentary data indicate the opposite behavior; i.e., low-lying resonances at ~ 10-20 eV.

minor. It is quickly apparent that the accuracy of radioactivity and afterheat calculations is limited almost entirely by the cross-section data uncertainties, especially for the $^{94}Nb(n,\gamma)$ reaction; errors due to angular quadrature and other numerical approximations are relatively minor.

3. Calculational Results

3.1 Radioactivity and Biological Hazard Potential (BHP)

The radioactivity induced by neutron transmutations depends on the blanket structural material, the wall loading (I_w), the operating time (T), and the time after shutdown (t_s). Although this radioactivity is conventionally expressed as either Q (Ci/Wt y) or A(Ci/Wt), these quantities have little technical significance, in that the induced radioactivity presents either a biological hazard (in the short- or long-run) or a cooling problem. The latter concern is best reflected in terms of the fraction, P/P_o, of the operating power which is represented by decay heat and is treated in the following Section 3.2. The biological hazard is most conveniently measured in terms of a biological hazard potential, BHP, defined as the ratio of A(Ci/Wt) to the maximum permissible concentration, MPC (Ci/km^3).* The principal usefulness of the BHP lies in its comparative function, and a physical significance should not be given to the absolute value of the BHP, since important properties like volatility, chemical state, and source distribution are not specified. The radioactivity and afterheat calculations are based on pure alloys, and the effects of impurities at the levels found in commercial alloys may be nontrivial. Incorporation of impurity effects, however, is beyond the scope of the present study.

Figure 1 compares A(Ci/Wt) vs t_s for the RTPR with values reported for tokamak fusion reactors.[8,9,10] The BHP associated with fission products[23] and plutonium[24] are incorporated onto a summary plot of BHP vs t_s given in Fig. 2. Both figures indicate the dependence of radioactivity and BHP on operating time and wall loading. Detailed analyses of this dependence can be found in Ref. 25. The differences in radioactivity between fusion reactors results from compositional variations (location and quantities of graphite); the varying quantities of structural alloy incorporated within the blanket (the more complex structure in the RTPR blanket requires ~ 6% volume of structure compared to ~ 1% for the ORNL tokamak); and differences in wall loading. Additional difference between fusion reactors arise because of the varying calculational bases selected for particular designs in incorporating specific radioisotopes into analyses of activation chains. For instance, the Wisconsin study[10] neglects the long-lived ^{94}Nb isotope in the Nb-1%Zr analysis and the ORNL study does not allow for a Ti alloying continuent, and thus the isotopes ^{45}Ca and ^{46}Sc, in the vanadium calculations. The ^{45}Ca and ^{46}Sc isotopes, although a small contributor to A(Ci/Wt), have a low MPC and therefore contribute most of the BHP. A comparison of the V (tokamak) curve with the V-20%Ti (RTPR) curve in Fig. 2 (once these curves are normalized to the same volume percent of structural materials) clearly illustrates the effects of Ti alloy additions on the BHP for vanadium. The radiological advantage of vanadium will almost certainly be further diminished if other low-level impurity and alloying constituents are taken into account.

---

*MPC's are given for air and water according[22] to whether i) the isotope is in a soluble or insoluble form, and ii) the release is into a controlled (40 hr/wk exposure) or an uncontrolled (168 hr/wk exposure) area. These MPC's pertain to individual doses and must be reduced by a factor of 3 when applied to a suitable sample of the exposed population. To assure an unambiguous comparison, all MPC's used herein apply to individual exposures in uncontrolled areas, and the smaller between soluble and insoluble values is used. MPC's quoted are for air concentrations. MPC values not found in Ref. 22 were calculated by J. W. Healy (Los Alamos Scientific Laboratory, personal communication, 1974).

Increased wall loading generally results in higher short-term activation (Ci/Wt) of the niobium structure as a result of second-order reactions which lead to ^{95,95m}Nb. The long-term activation for a given value of T, however, is seen to decrease with increasing I_w, as a result of the burnout of the long-lived ^{94}Nb and its parent ^{93}Nb.

Because the copper compression coils are in close proximity to the blanket in the RTPR design, the neutron flux level and subsequent activation will be significant. Figure 1 gives the decay of copper activity for typical RTPR conditions, and Table I summarizes the RTPR radioactivity and biological hazard potential for the copper compression coil at shutdown for the design wall loading (2.0 MW/m^2) as a function of operating time. The isotopes ^{60}Co($t_{1/2}$ = 5.272 y) and ^{63}Ni ($t_{1/2}$ = 100 y) represent the major long-term radwaste concern (0.5% of the total copper activity at shutdown for T = 10 y). The ^{63}Ni activity, although long lived, emits only a soft (E_{max} = 0.07 MeV) beta. The total copper activity is 20% of the Nb-1%Zr activity (I_w = 2.0 MW/m^2, T = 5 y) at shutdown, although the short-lived nature of the dominant copper activity (Table I) presents mainly an afterheat problem rather than a radiological hazard. A comparison of the BHP's for I_w = 2.0 MW/m^2 in Tables I and III does show, however, that the copper coils have slightly higher values than a V-20%Ti blanket. In the case of a Nb-1%Zr blanket the copper coils contribute only about 5% of the biological hazard potential.

The dependence of the blanket radioactivity (and afterheat) on T and I_w was indicated by the results presented in Figs. 1 and 2. Tables II and III illustrate the effect of wall loading, I_w, and operating time, T, on the Nb-1%Zr and V-20%Ti radioactivity biological hazard potential, and afterheat. The strong dependence on I_w of the ^{95,95m}Nb activity is immediately evident from Table II with ^{95}Nb dominating the activity at the higher values of I_w. The less dramatic effect of ^{93,94}Nb burnout is also observed. Figure 3 summarizes the dependence of A(Ci/Wt), Q(Ci/Wt y), and P/P$_o$ on the operating time, T, for various wall loadings, I_w, in the Nb-1%Zr RTPR. As was discussed previously, calculations of the ^{95,95m}Nb activities are subject to considerable error caused by uncertainty in the ^{94}Nb radiative capture cross section. The high activities at large values of I_w may in fact be illusory if ^{94}Nb capture resonances are predominately low lying. Table II clearly illustrates the strong effect of ^{95}Nb activity on the BHP. Even though the ^{94m}Nb activity (Ci/Wt) dominates for $I_w \lesssim 2.0$ MW/m^2, its BHP is negligible relative to that of ^{95}Nb. Thus, the total BHP increases much more rapidly with wall loading than does A(Ci/Wt).

Studies of the variation of radioactivity from V-20%Ti with wall loading were also performed, with less pronounced differences (Table III). Variations in total Ci/Wt, BHP, and P/P$_o$ are not significant (at most 3%). Therefore, the second-order reactions on ^{45}Sc, ^{50}Ti, ^{50}V and ^{52}Cr (produced by first-order reactions on stable nuclei of Ti or V) are shown to be of minor importance, unlike the possible case with ^{94}Nb. Consecutive (n,2n) reaction on ^{46}Ti to produce ^{44}Ti (47 y) were assumed to be a negligible contributor to the radioactivity. The first six radioisotopes in Table III are those considered by Steiner[8] for a pure vanadium structure; the remaining six are principally products of titanium activation. Approximately 75% of the ^{47}Sc production in the RTPR, however, comes from the ^{49}Ti(n,n'p) reactions, not from ^{50}V(n,α) or ^{51}V(n,n'α) reactions. As can be seen in Table III, the ^{45}Ca and ^{46}Sc will be the dominant contributors to BHP for several (6-10) years after shutdown, because of their high initial BHP and relatively long half lives. The only longer-lived isotope, 331-d ^{46}V, has an initial BHP at least two orders of magnitude lower than ^{45}Ca or ^{46}Sc for any wall loading considered.

On the basis of the foregoing results, the dependence of Q(Ci/Wt y), A(Ci/Wt), and BHP(km^3/Wt) on I_w, T, and t_s for Nb-1%Zr is complicated by second-order production reactions, burnout of stable ^{93}Nb and radioactive isotopes, and

the natural variations in half-life and MPC's. As evidenced from the data presented on Fig. 3 different costs are accrued (i.e., total curies of activity) for the same apparent benefit (i.e., Wt-y of energy received) depending on the individual values of wall loading (directly relatable to power) and operating time. For the case where the activity at shutdown is comprised primarily of short-lived isotopes (i.e., ^{94m}Nb and ^{92m}Nb), this situation is best described by plotting the "cost-benefit ratio" A(Ci/Wt) vs the total energy delivered (GWt y). Figure 4 illustrates this correlation at $t_s = 0$, and this correlation is independent of wall loading in the range 0.2 to 6.7 MW/m^2 (360 to 12,000 MWt for the RTPR). The "activity cost" (Ci) per unit of thermal power (Wt) derived from a given blanket structure increases with increasing energy (GWt y) as second order reactions build in activity. As the derived energy increases, the benefit of activity burnout is realized and the curve shows a maximum. Specifically, this maximum is a result of the burnout of ^{93}Nb and ^{94}Nb and occurs at unrealistically large first-wall neutron fluences (corresponding to transmutation of ~ 20% of the original niobium), but not unrealistic for recycled niobium.

Figure 4 corresponds to a "cost-benefit" ratio which is most applicable at shutdown ($t_s = 0$). Since the real cost of the induced radioactivity must often be attributed to long-term storage requirements, the dependence of the "cost-benefit" ratio, α(Ci/Wt y), on total delivered energy (GWt y) at long shutdown times is of interest; this behavior is illustrated in Fig. 5. The quantity α(Ci/Wt y) represents a "cost-benefit" ratio which is more useful for large values of t_s and eventually becomes independent of wall loading for long times after shutdown. The isotope ^{94}Nb represents the major long-term activity, and the decrease of α(Ci/Wt y) with delivered energy (GWt y) for a given large value of t_s reflects the burnout of this activity.

3.2 Nuclear Afterheat

Nuclear afterheat represents a concern for both fission and fusion power reactors in event of a loss-of-cooling accident. In assessing the nuclear afterheat problem, primary consideration must be given to the fraction of the operating thermal power which is represented by nuclear afterheat, P/P_o, as well as the specific power (MW/m^3) generated within the blanket by the afterheat. The dependence of P/P_o on wall loading, operating time, and material have been summarized for the RTPR in Tables II-III. The lifetime of the copper coils is expected to be 2-4 times that of the blanket, but their afterheat power saturates in a few days and changes < 1% for up to 20 years operation (cf. Table I).

A comparison of the time dependence of P/P_o calculated for the RTPR is made with other fusion reactor concepts as well as with a representative fission reactor in Fig. 6. The fission product curve from Ref. 26 is for the thermal fission of ^{235}U, although the afterheat resulting from the fast fission of ^{239}Pu is shown in Ref. 27 to differ little (< 10% for 10^2 s < t_s < 2 y) from the thermal fission of ^{235}U.

For the case of a loss-of-cooling accident interest focuses on the magnitude of P/P_o for approximately the first day after the accident. Although P/P_o for a fission reactor is of the same order as for the RTPR, (the RTPR contains ~ 6 times more structure than the other fusion reactor concepts considered) the difference in specific afterheat power can be significant. The RTPR generates 3 600 MWt in a 718 m^3 blanket, which corresponds to an operating power density of 5.01 MW/m^3 (of blanket). The volume fraction of Nb in the RTPR blanket is 6.1 v/o (44 m^3), and all afterheat can be conservatively assumed to be deposited within the niobium. This assumption leads to an average afterheat power density of 0.81 MW/m^3 (of niobium) shortly after shutdown. The peak-to-average afterheat

power ratio in the niobium is ~ 2.3,* with the maximum occurring at the first wall. Also shown on Fig. 6 is P/P_o for the RTPR with V-20%Ti substituted for Nb-1%Zr in the blanket. The difference for V or V-20%Ti between the ORNL and the UWMAK-I tokamak is a result of considerably less structural metal in the ORNL design and the incorporation of stainless steel moderator in the UWMAK design. The Westinghouse LMFBR demonstration plant[24] is selected for comparison of nuclear afterheat power densities with the RTPR. The Westinghouse LMFBR demonstration plant will generate 790 MWt (330 MWe) in a 2.183 m^3 active core volume. The UO_2/PuO_2 (~ 22 w/o PuO_2) fuel amounts to 36.0 v/o of the active core volume. The corresponding operating power density is 360 MW/m^3 (of active core volume) or 1000 MW/m^3 (of fuel). The afterheat power density at ~ 10 s after shutdown for this fission reactor, therefore, amounts to ~ 50 MW/m^3 (of fuel) or a factor of ~ 60 greater than the RTPR (and even a greater fraction for other fusion reactor designs). Detailed heat-transfer calculations must be made which account for post-accident core configurations before the significance of this difference in afterheat power density can be accurately evaluated. New data on the $^{94}Nb(n,\gamma)$ cross section will in all likelihood significantly reduce the calculated ^{95}Nb contribution to afterheat. Furthermore, more detailed calculations performed on fusion reactor designs which incorporate activities induced in the impurities found in commercially pure structural alloys may increase P/P_o for fusion reactors. However, fusion reactors as now envisioned are inherently low power density machines, and it is difficult to imagine afterheat problems in fusion reactors which are of the same order as the problems presently faced by fission reactors.

4. Conclusions and Summary

The foregoing analyses and results have given the major dependencies of radioactivity [A(Ci/Wt), α(Ci/Wt y), and BHP(km^3/Wt)] and nuclear afterheat (P/P_o) on material, wall loading (I_w), operating time (T) and shutdown time (t_s) variables. This study is far from complete, although the results presented herein do represent a portion of the state-of-the-art knowledge upon which near-term decisions will be made in fusion reactor design activities. Conclusions which have pertinence to this decision process are summarized below.

i) Impurity activation in both structural and nonstructural blanket components may have a significant influence on the values of BHP and, to a lesser extent, P/P_o computed herein. A study of the influence of impurities should be incorporated into the second round of fusion reactor design exercises.

ii) The cross section data used in these analyses are inadequate for radiological/afterheat assessments with greater than ~ 25% accuracy (~ factor of 2 for $^{95,95m}Nb$); for this reason the results and conclusions presented herein should be viewed as preliminary estimates. Much more work and refinement must be done before these kinds of calculation for fusion reactors will be on an equal footing with similar estimates made for fission reactors. This singular fact should be kept in mind when making radiological fission/fusion comparisons. Estimates of $^{95,95m}Nb$ activity most likely err on the high side, overpredicting BHP and P/P_o, while ^{94}Nb predictions probably err on the low side.

---

*This value of peak-to-average afterheat ratio is much less than might be inferred from the attenuation of the total neutron flux through the blanket. Most of the activation which contributes to afterheat results from successive neutron captures ($^{93}Nb \rightarrow {}^{94}Nb \rightarrow {}^{95}Nb$) and is therefore most dependent upon the low energy neutron flux.

iii) The large contribution to the total radioactivity of Nb-1%Zr fusion reactors by second-order neutron absorptions renders higher radioactivities (Ci/Wt or Ci/Wt y) for higher wall loadings at short times after shutdown (< 1 y) for a given operating time. This dependency is reversed at long decay times (> 100 y) because of the burnout of ^{93,94}Nb. Therefore, a long-term advantage exists for higher wall loadings as far as possible storage requirements are concerned.

iv) The sensitivity of A(Ci/Wt) and BHP(km^3/Wt) to the details of a given fusion reactor design was demonstrated. This sensitivity is caused by differences in the total quantity of structural material believed acceptable for a given design configuration, the relative complexity of a given blanket design, the location of neutron moderating materials within the blanket relative to resonance absorbing materials, differences in wall loading, and the neutron cross sections used in a given analysis.

v) The V-20%Ti alloy exhibits an order of magnitude less short-term radioactivity relative to Nb-1%Zr alloy; the long-term activity (> 100 y) for V-20%Ti is zero for the isotopes studied. The radiological advantage of V-20%Ti will almost certainly be diminished if low-level impurities and alloying constituents are taken into account by future analyses. The addition of 20%Ti to V does not significantly alter the radioactivity or afterheat, but increases the BHP appreciably. Use of copper magnetic coils in the RTPR design will cause the BHP of the coils to exceed that of a pure V-20%Ti blanket.

vi) Because of the close proximity of the copper magnetic coils to the RTPR blanket, considerable neutron activation of the copper is expected. The major portion of this activity is short-lived (≤ 12.74 h) and therefore presents more of an afterheat problem than a radiological (storage) problem; the copper activity is ~ 20% of the Nb-1%Zr activity (Ci/Wt) and ~ 5% of the Nb-1%Zr biological hazard potential at shutdown (I_w = 2.0 MW/m^2, T = 5 yr). The isotope ^{63}Ni ($t_{1/2}$ = 100 y) represents a major long-term contributor to the radioactivity from a radwaste point-of-view, although this situation may change if impurities found in commercially pure copper (or copper alloy) are incorporated into the analysis. The 5.272-y ^{60}Co may be the most important contributor to maintenance and recycling problems for the coils. Employing aluminum coils should reduce the induced activity by orders of magnitude.

vii) The general dependence of radioactivity and afterheat on wall loading and operating time is shown for V-20%Ti and Nb-1%Zr structural alloys. For V-20%Ti the second order reactions on ^{45}Sc, ^{50}Ti, ^{50}V, and ^{52}Cr are shown to be of minor importance (< 3%), unlike the case for ^{94}Nb in the Nb-1%Zr RTPR.

viii) The dependence of P/P_o on the peculiarities of the fusion reactor design is appreciable for the reasons cited in iv) above; the RTPR has values which are of the same order reported for fission reactors. The afterheat power density, however, is expected to be one to two orders-of-magnitude below that for a "fast" fission reactor. This situation results from the low power density which is inherent to magnetically confined CTR's. For this reason afterheat in conjunction with loss-of-coolant or coolant-flow is not expected to be a major concern for fusion reactors. Detailed heat transfer calculations, however, must be performed in conjunction with a realistic accident scenario before analysis of the loss-of-cooling accident is on the same quantitative footing as for fission reactors.

ix) The BHP for the fusion reactor cases considered herein is considerably below that for a fission reactor of equivalent power. Although the BHP is a comparative quantity, and little physical significance can meaningfully be attributed directly to this quantity, even the comparative quality of the BHP has limitations. For instance, the radioactivity expected to be generated from fusion reactors will chemically be of a refractory nature, unlike the volatile nature of biologically hazardous fission products. Therefore, even if the BHP values predicted fusion and fission to be of the same order, the chemistry of the respective activities predicts a less stringent storage task for the fusion radwaste. This conclusion, however, is subject to the uncertainties listed in i) and ii) above. Additionally, the structural "radwaste" from a fusion power plant is in a metallurgical form which is amenable to reclamation and recycling; in fact if Nb-1%Zr is used recycling of the blanket structure appears almost certain.[1]

x) For fusion reactors constructed from Nb-1%Zr alloy, the isotope ^{94}Nb (2.0×10^4 y) is a major long-term contribution to the BHP, which for $t_s > 400$ y exceeds the fission-products component of the BHP for fission reactors. The BHP's of ^{94}Nb and fission products are, however, always greatly overshadowed by that for the transuranium elements (primarily plutonium) in fission reactors.

5. References

1. T. A. Coultas, J. E. Draley, V. A. Maroni, R. A. Krakowski, "An Engineering Design of a Reference Theta-Pinch Reactor, RTPR," Vol. II; An Environmental Impact Study, USAEC Rept. ANL-8019/LA-5336, April 1974.

2. R. A. Krakowski, F. L. Ribe, T. A. Coultas, A. J. Hatch, "An Engineering Design of a Reference Theta-Pinch Reactor," Vol. 1, USAEC Rept. ANL-8019/LA-5336, Feb. 1974.

3. A. P. Fraas, H. Postma, "Preliminary Appraisal of the Hazards Problems of a D-T Fusion Reactor Power Plant," USAEC Rept. ORNL-TM-2822, (1970).

4. Donald J. Dudziak, "A Technical Note on D-T Fusion Reactor Afterheat," Nucl. Tech., 10, 391, (1971).

5. D. Steiner, "The Neutron-Induced Activity and Decay Power of the Niobium Structure of a D-T Fusion Reactor Blanket," USAEC Rept. ORNL-TM-3094 (1970).

6. S. Blow, "Some Features of the Behavior of Structural Materials in a Possible Fusion Reactor Blanket," J. Brit. Nucl. En. Soc., 11, 4, 371, (1972).

7. D. Steiner, A. P. Fraas, "Preliminary Observations on the Radiological Implications of Fusion Power," Nucl. Safety, 13, 5, 353 (1972).

8. D. Steiner, "The Nuclear Performance of Vanadium as a Structural Material in Fusion Reactor Blankets," USAEC Report ORNL-TM-4353 (1973).

9. W. F. Vogelsang, G. L. Kulcinski, R. G. Lott, and T. Y. Sung, "Transmutation Effects in CTR Blankets," Trans. Am. Nucl. Soc., 17, 138 (1973).

10. B. Badger, et al., "UWMAK-I, A Wisconsin Toroidal Fusion Reactor Design," USAEC Report, UWFDM-68, Vol. 1 (1973).

11. F. L. Ribe, T. A. Oliphant, W. E. Quinn, "Feasibility Study of a Pulsed Thermonuclear Reactor," USAEC Report LA-3294-MS (1965).

12. G. I. Bell, W. H. Borkenhagen, F. L. Ribe, "Feasibility Studies of Pulsed High-β Fusion Reactors," p. 242, Proc. BNES Conf. on Nucl. Fusion Reactors, UKAEA Culham Laboratory, (Sept. 17-19, 1969).

13. S. C. Burnett, W. R. Ellis, T. A. Oliphant, F. L. Ribe, "A Reference Theta-Pinch Reactor (RTPR): A Study of a Pulsed High-Beta Fusion Reactor Based on the Theta Pinch," USAEC Report LA-5121-MS (1972).

14. G. I. Bell, "Neutronic Blanket Calculations for Thermonuclear Reactors," USAEC Report LA-3385-MS (1965).

15. Donald J. Dudziak, "Neutronic Characteristics of a Reference Theta-Pinch Reactor (RTPR) Blanket," Los Alamos Scientific Laboratory Report (to be published).

16. Donald J. Dudziak, "Transmutation and Atom Displacement Rates in a Reference Theta-Pinch Reactor," First Topical Meeting on the Technology of Controlled Nuclear Fusion, April 16-18, 1974.

17. K. D. Lathrop, "DTF-IV, A FORTRAN-IV Program for Solving the Multigroup Transport Equation with Anisotropic Scattering," USAEC Rept. LA-3373 (1965).

18. D. W. Muir and R. J. LaBauve, LASL, private communication (1972).

19. J. R. Stehn, et al "Neutron Cross Sections," USAEC Rept. BNL-325, 2nd ed., Supp. #2 (1964).

20. F. Hegedus "Detecteur de Fluence de Neutrons Rapides Utilisant la Reaction ^{93}Nb (n,n') ^{93m}Nb," USAEC Rept. FRNC-TH-228 (1972) [also, dissertation al'Universite Louis Pasteur de Strasbourg].

21. N. E. Holden, F. W. Walker, "Chart of the Nuclides, 11th Ed.," April 1972.

22. USAEC Manual of Standards for Radiation Protection, Chart 0524, Nov. 18, 1968 on USAEC Rules and Regulations, Title 10, Atomic Energy Supplement, Rec. 10, 1969.

23. W. B. Cottrell, A. W. Savolainen, "U.S. Reactor Containment Technology," USAEC Rept. ORNL-NSIC-5, p 4.2-4.3, (1965).

24. "Final Report, Project Definition Phase, 4th Round Demonstration Plant Program," Vol. I., Westinghouse Electric Corp., Dec. 1970.

25. Donald J. Dudziak, R. A. Krakowski, "Radioactivity Induced in the Reference Theta-Pinch Reactor (RTPR)," submitted to Nucl. Appl.

26. K. Shure, D. J. Dudziak, "Calculating Energy Released by Fission Products," Trans. Am. Nucl. Soc., 4, 1, 30, (1961). See also USAEC Rept. WAPD-T-1309.

27. M. E. Battat, D. J. Dudziak, H. R. Hicks, "Fission Product Energy Release and Inventory from ^{239}Pu Fast Fission," USAEC Rept. LA-3954 (1967).

TABLE I

RTPR RADIOACTIVITY AT SHUTDOWN IN COPPER VS OPERATING TIME

(I_w = 2.0 MW/m^2, the reference case)

Isotope	$t_{1/2}$	Activity (Ci/Wt) T = 5 y	Activity (Ci/Wt) T = 10 y	Activity (Ci/Wt) T = 20 y	BHP (km^3/Wt) T = 20 y
^{60}Co	5.72 y	1.75×10^{-3}	2.66×10^{-3}	3.38×10^{-3}	1.13×10^{-2}
^{62}Co	13.9 m	1.63×10^{-3}	1.63×10^{-3}	1.63×10^{-3}	8.15×10^{-7}
^{63}Ni	100 y	7.48×10^{-4}	1.47×10^{-3}	2.84×10^{-3}	1.42×10^{-3}
^{65}Ni	2.520 h	9.54×10^{-4}	9.54×10^{-4}	9.54×10^{-4}	4.77×10^{-5}
^{62}Cu	9.78 m	0.0262	0.0262	0.0262	8.73×10^{-6}
^{64}Cu	12.74 h	0.649	0.649	0.648	1.62×10^{-2}
^{66}Cu	5.10 m	0.108	0.108	0.108	1.08×10^{-5}
TOTALS - Ci/Wt		0.7883	0.7899	0.7910	BHP: 0.0290
Ci/Wt y		0.1577	0.07899	0.03955	
P/P_o (%)		0.245	0.246	0.247	

TABLE II. RTPR AFTERHEAT AND RADIOACTIVITY AT SHUTDOWN IN Nb-1%Zr VS WALL LOADING (T = FIVE YEARS)

					Reference Design			
	I_w = 0.2		I_w = 0.5		I_w = 2.0		I_w = 6.7	
Isotope	Ci/Wt	BHP	Ci/Wt	BHP	Ci/Wt	BHP	Ci/Wt	BHP
^{92}Nb(2×10^{7} y)	7.42×10^{-8}	2.12×10^{-10}	7.41×10^{-8}	2.12×10^{-10}	7.36×10^{-8}	2.1×10^{-10}	7.19×10^{-8}	2.05×10^{-10}
^{92m}Nb(10.13d)	0.288	7.78×10^{-4}	0.288	7.78×10^{-4}	0.287	7.76×10^{-4}	0.282	7.62×10^{-4}
^{93m}Nb(12 y)	0.0609	0.0152	0.0608	0.0152	0.0606	0.0152	0.0601	0.0150
^{94}Nb(2.0×10^{4}y)	5.98×10^{-4}	2.99×10^{-4}	5.68×10^{-4}	2.84×10^{-4}	4.45×10^{-4}	2.22×10^{-4}	2.39×10^{-4}	1.20×10^{-4}
^{94m}Nb(6.26 m)	1.78	8.90×10^{-6}	1.78	8.90×10^{-6}	1.75	8.79×10^{-6}	1.67	8.35×10^{-6}
^{95}Nb(35.1d)	0.213	0.0710	0.503	0.168	1.55	0.517	2.61	0.870
^{95m}Nb(3.61d)	0.0425	1.52×10^{-4}	0.101	3.61×10^{-4}	0.311	1.11×10^{-3}	0.521	1.86×10^{-3}
^{89}Sr(50.5d)	-	-	-	-	1.04×10^{-4}	3.47×10^{-4}	3.25×10^{-4}	1.08×10^{-3}
^{90}Sr(29 y)	-	-	-	-	4.67×10^{-7}	1.56×10^{-5}	1.42×10^{-6}	4.73×10^{-5}
^{90}Y(64 h)	-	-	-	-	6.78×10^{-3}	2.26×10^{-3}	6.78×10^{-3}	2.26×10^{-3}
^{90m}Y(3.19 h)	-	-	-	-	$<6.78\times10^{-3}$	$<9.68\times10^{-6}$	$<6.78\times10^{-3}$	$<9.68\times10^{-6}$
^{93}Zr(9.5×10^{5}y)	-	-	-	-	8.97×10^{-8}	2.24×10^{-8}	8.96×10^{-8}	2.24×10^{-8}
TOTALS	2.38	0.0874	2.73	0.185	3.96	0.534	5.14	0.889
P/P_o(%)	0.312		0.459		0.990		1.52	

TABLE III. RTPR AFTERHEAT AND RADIOACTIVITY AT SHUTDOWN IN V-20%Ti VS WALL LOADING (T = FIVE YEARS).

		Reference Design					
		I_w = 0.5 MW/m^2		I_w = 2.0 MW/m^2		I_w = 6.7 MW/m^2	
Isotope	$t_{1/2}$	Ci/Wt	BHP	Ci/Wt	BHP	Ci/Wt	BHP
^{47}Sc	3.41 d	3.61×10^{-3}	1.80×10^{-4}	3.83×10^{-3}	1.92×10^{-4}	4.45×10^{-3}	2.22×10^{-4}
^{48}Sc	43.7 h	0.0228	4.56×10^{-3}	0.0226	4.52×10^{-3}	0.0226	4.52×10^{-3}
^{51}Ti	5.76 m	0.0467	5.49×10^{-5}	0.0467	5.49×10^{-5}	0.0466	5.48×10^{-5}
^{49}V	331 d	1.15×10^{-3}	4.60×10^{-6}	4.58×10^{-3}	1.83×10^{-5}	0.0147	5.88×10^{-5}
^{52}V	3.755 m	0.370	1.06×10^{-3}	0.369	1.05×10^{-3}	0.366	1.05×10^{-3}
^{51}Cr	27.71 d	9.03×10^{-5}	1.13×10^{-6}	3.62×10^{-4}	4.52×10^{-6}	1.20×10^{-3}	1.50×10^{-5}
SUBTOTAL		0.444	5.86×10^{-3}	0.447	5.84×10^{-3}	0.456	5.91×10^{-3}
^{45}Ca	163 d	4.66×10^{-3}	4.66×10^{-3}	4.66×10^{-3}	4.66×10^{-3}	4.65×10^{-3}	4.65×10^{-3}
^{47}Ca	4.54 d	6.14×10^{-5}	1.02×10^{-5}	6.56×10^{-5}	1.09×10^{-5}	7.88×10^{-5}	1.31×10^{-5}
^{46}Sc	83.8 d	5.07×10^{-3}	6.33×10^{-3}	5.10×10^{-3}	6.38×10^{-3}	5.15×10^{-3}	6.44×10^{-3}
^{49}Sc	57.3 m	4.44×10^{-4}	3.42×10^{-7}	4.44×10^{-4}	3.42×10^{-7}	4.43×10^{-4}	3.41×10^{-7}
^{50}Sc	1.71 m	1.54×10^{-4}	1.40×10^{-6}	1.64×10^{-4}	1.49×10^{-6}	1.96×10^{-4}	1.78×10^{-6}
^{45}Ti	3.078 h	2.08×10^{-4}	6.12×10^{-7}	2.08×10^{-4}	6.12×10^{-7}	2.08×10^{-4}	6.12×10^{-7}
TOTAL		0.455	0.0169	0.458	0.0169	0.466	0.0170
P/P_o(%)		0.554		0.553		0.549	

Figure and Table Captions

Fig. 1. Intercomparison of A(Ci/Wt) for various fusion and fission reactor concepts.
(a) reference 23
(b) reference 8
(c) reference 9, 10

Fig. 2. Intercomparison of BHP(km^3/Wt) for various fusion and fission reactor concepts.
(a) reference 24
(b) reference 23
(c) reference 9, 10
(d) reference 8

Fig. 3. Summary of the dependence of A(Ci/Wt), α(Ci/Wt y), and P/P_o on operating time, T, at various wall loadings, I_w, for the Nb-1%Zr RTPR and $t_s = 0.0$.

Fig. 4. Dependence of A(Ci/Wt) on $P_{TH}T$ (GWt y) for $t_s = 0.0$.

Fig. 5. Dependence of α(Ci/Wt y) on $P_{TH}T$ (GWt y) for various values of t_s.

Fig. 6. Intercomparison of nuclear afterheat, P/P_o, for various fusion and fission reactor concepts.
(a) reference 26
(b) reference 8
(c) reference 7
(d) reference 9, 10

Table I. RTPR Radioactivity at Shutdown in Copper vs Operating Time ($I_w = 2.0$ MW/m^2, the reference case).

Table II. RTPR Afterheat and Radioactivity at Shutdown in Nb-1%Zr vs Wall Loading (T = 5 years).

Table III. RTPR Afterheat and Radioactivity at Shutdown in V-20%Ti vs Wall Loading (T = 5 years).

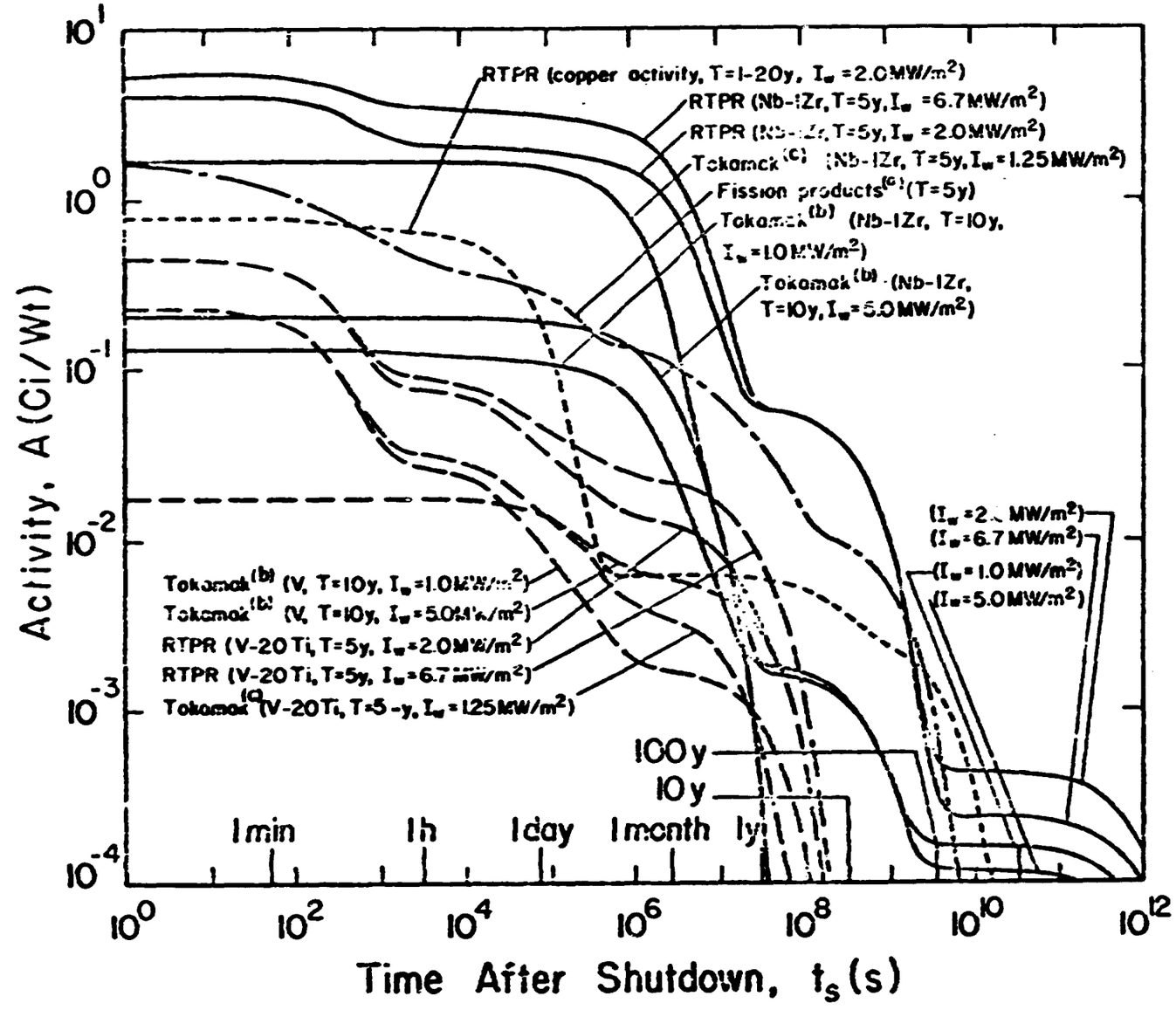

Fig. 1. Intercomparison of A(Ci/Wt) for various fusion and fission reactor concepts.
(a) reference 23
(b) reference 8
(c) reference 9, 10

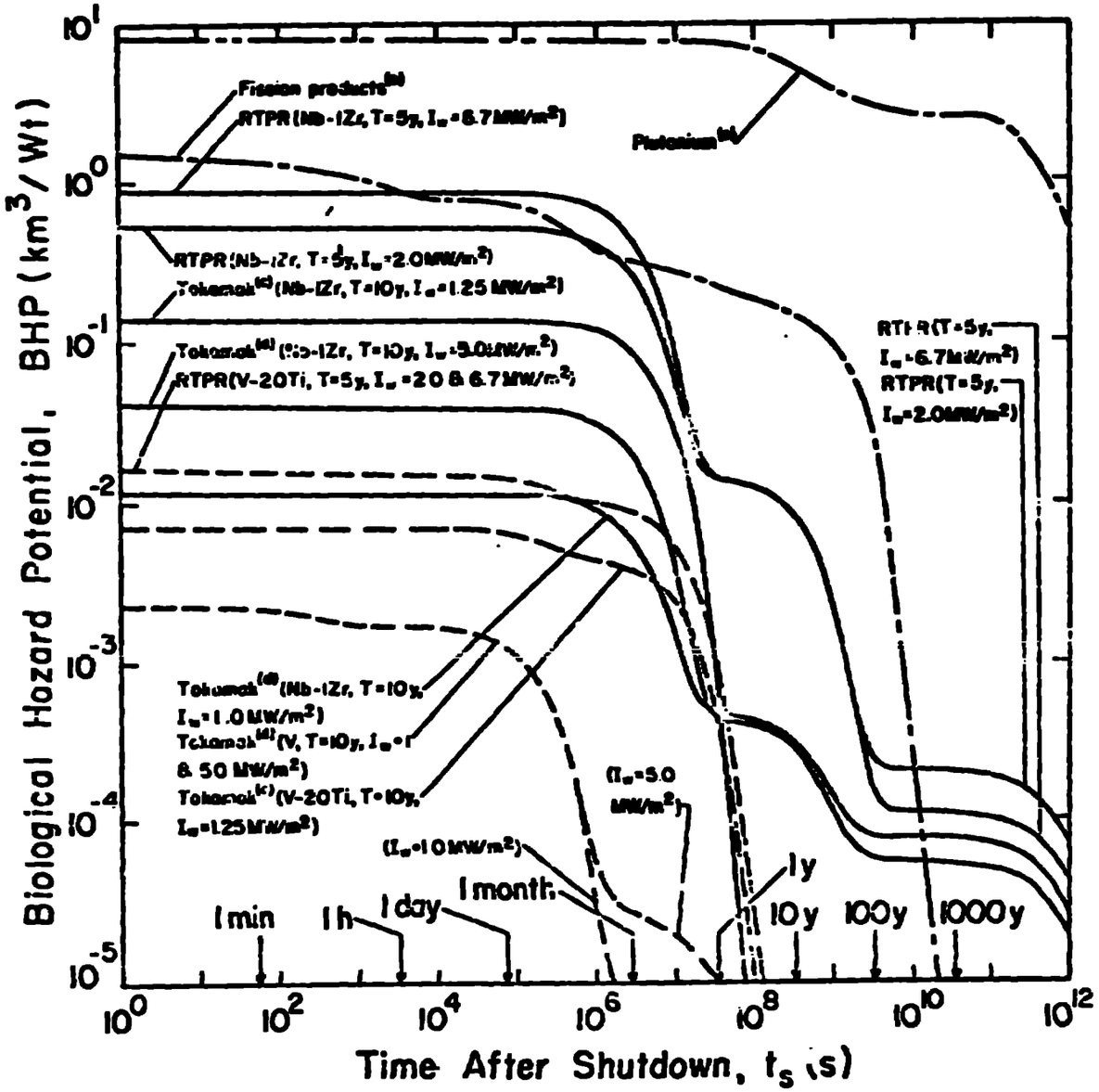

Fig. 2. Intercomparison of BHP(km^3/Wt) for various fusion and fission reactor concepts.
(a) reference 24
(b) reference 23
(c) reference 9, 10
(d) reference 8

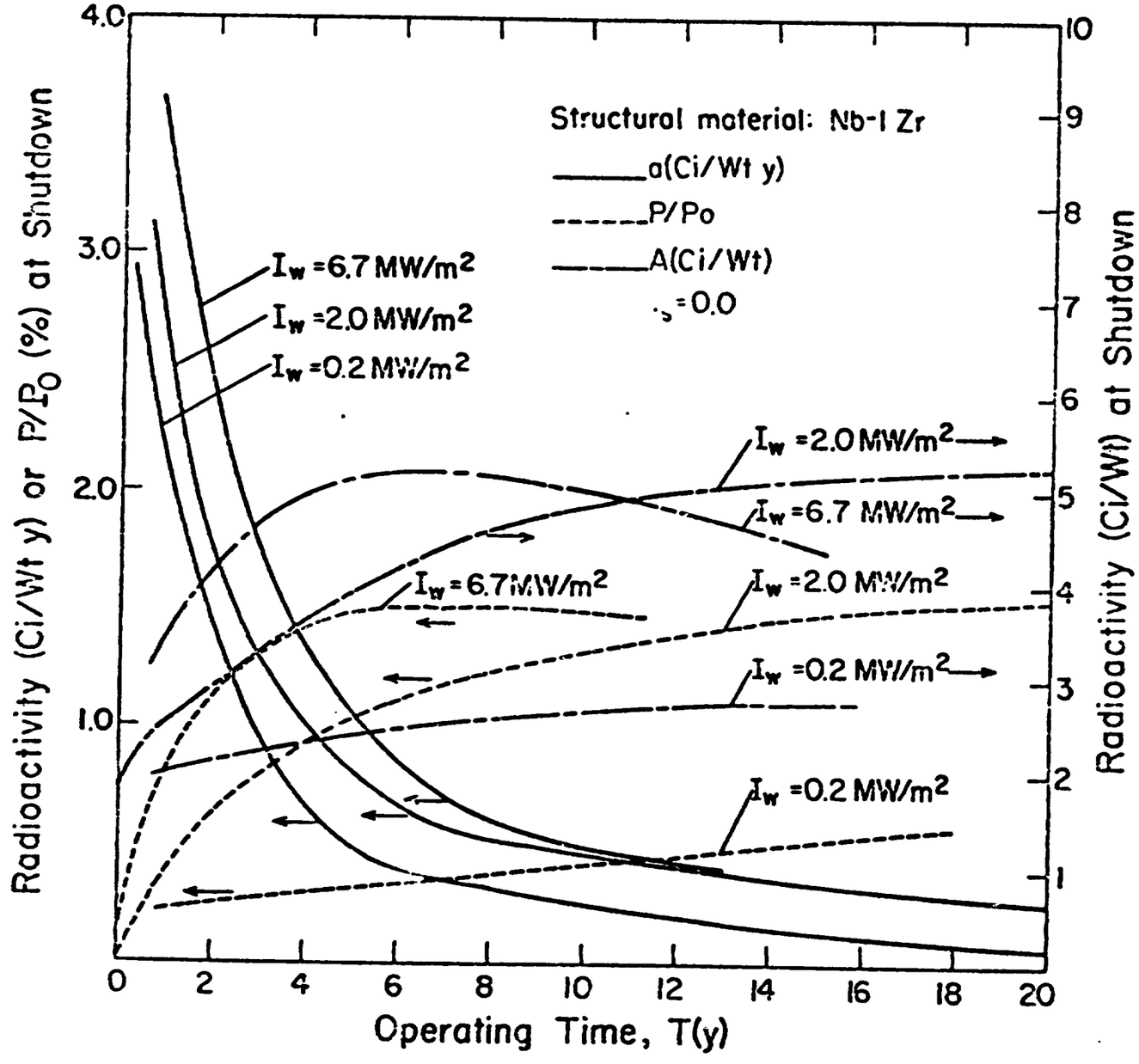

Fig. 3. Summary of the dependence of A(Ci/Wt), α(Ci/Wt y), and P/P_o on operating time, T, at various wall loadings, I_w, for the Nb-1%Zr RTPR and t_o = 0.0.

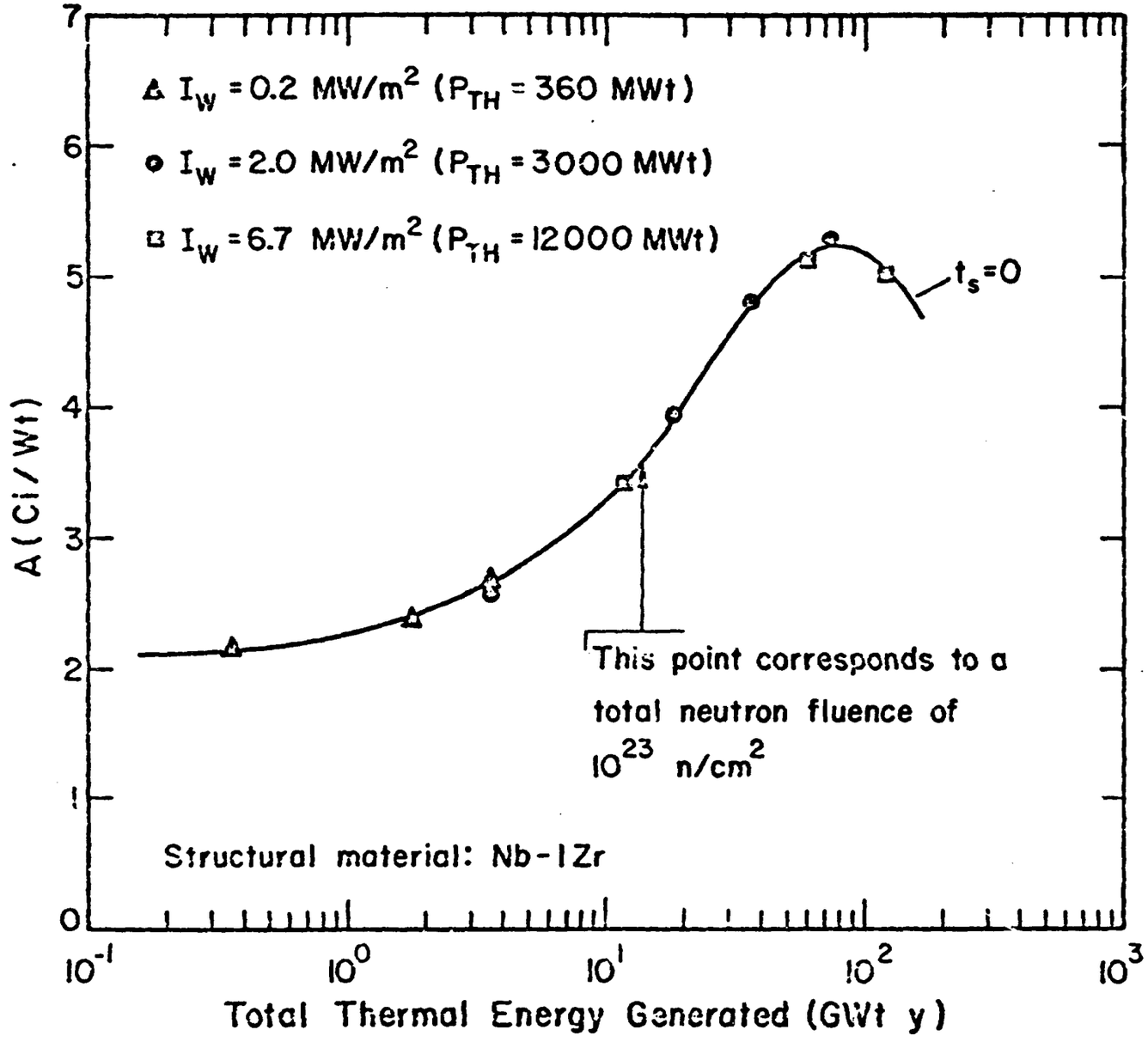

Fig. 4. Dependence of A(Ci/Wt) on $P_{TH}T$ (GWt y) for t_s = 0.0.

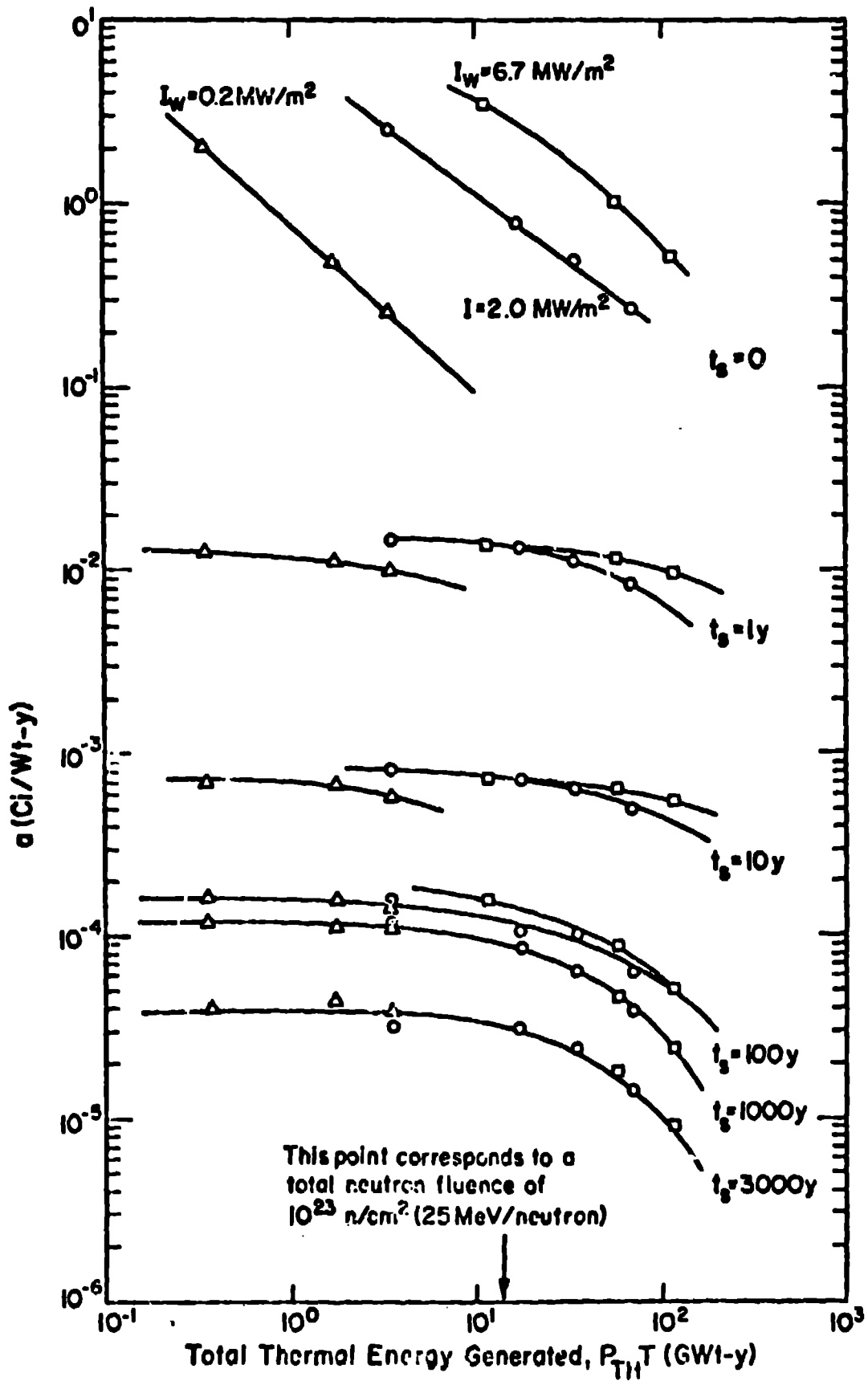

Fig. 5. Dependence of Q(Ci/Wt y) on $P_{TH}T$ (GWt y) for various values of t_s.

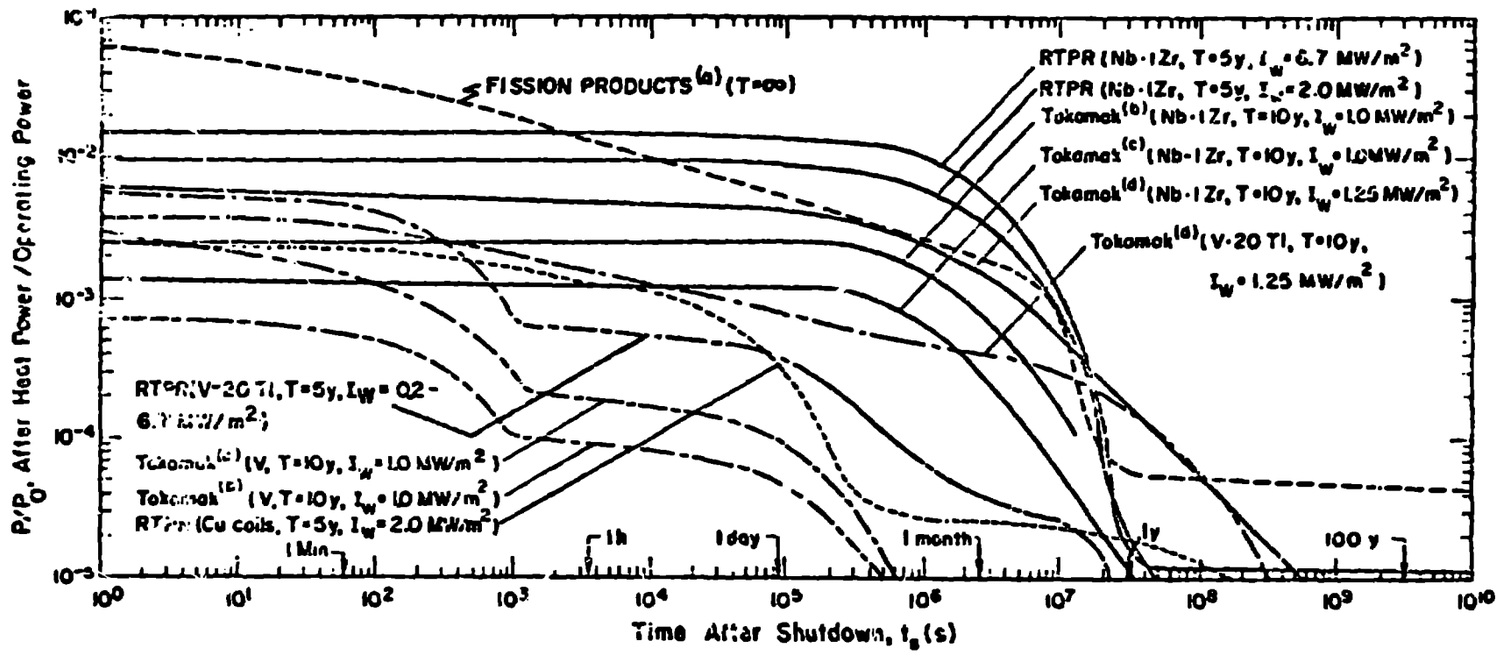

Fig. 6. Intercomparison of nuclear afterheat, P/P_o, for various fusion and fission reactor concepts.
(a) reference 26
(b) reference 8
(c) reference 7
(d, reference 9, 10